Supramolecular surface functionalization via catechols for the improvement of cell-material interactions

Biomaterials Science

ARTICLE

Supramolecular surface functionalization via catechols for the improvement of cell-material interactions

Received 00th January 20xx,
Accepted 00th January 20xx

DOI: 10.1039/x0xx00000x

www.rsc.org/

Spaans, S.[a,b], Fransen, P. P. K. H.[a,c], Ippel, B. D.[a,b], Keizer, H. M.[a,d], Bax, N. A. M.[a,b], Bouten, C. V. C.[a,b], Dankers, P. Y. W.[a,b,c]

Optimization of cell-material interactions is crucial for the success of synthetic biomaterials in guiding tissue regeneration. To do so, catechol chemistry is often used to introduce adhesiveness into biomaterials. Here, a supramolecular approach based on ureido-pyrimidinone (UPy) modified polymers is combined with catechol chemistry in order to achieve improved cellular adhesion onto supramolecular biomaterials. UPy-modified hydrophobic polymers with non-cell adhesive properties are developed that can be bioactivated via a modular approach using UPy-modified catechols. It is shown that successful formulation of the UPy-catechol additive with the UPy-polymer results in surfaces that induce cardiomyocyte progenitor cell adhesion, cell spreading, and preservation of cardiac specific extracellular matrix production. Hence, by functionalizing supramolecular surfaces with catechol functionalities, an adhesive supramolecular biomaterial is developed that contains superior cell-adhesive properties and allows for the possibility to contribute to biomaterial-based regeneration.

Introduction

Materials and systems inspired by nature have shown great promise for the development of cell adhesive surfaces and biomedically applied adhesive glues.[1–3] Specifically, in the field of tissue engineering researchers have been inspired by the adhesive properties of marine mussels. Mussels show superior adhesion on wet surfaces through their byssal threads.[4] Within these threads, proteins containing the amino acid 3,4-dihydroxyphenylalanine (DOPA), are secreted in a spatially and temporally controlled manner which then form adhesive plaques in minutes.[5] The strong adhesive properties of these threads originate from catechol residues of DOPA, which have efficient and versatile cross-linking abilities. In reducing conditions, catechol residues can undergo various interactions, such as hydrogen bonding, electrostatic interactions or metal-catechol coordination.[6] Once exposed to oxygen, catechol residues are oxidized to reactive *o*-quinones. The *o*-quinones can then i) self-polymerize, ii) react with thiols or amines via Michael type addition or iii) react with amines via Schiff base reactions.

Many of these cross-linking abilities have contributed to the development of synthetic materials with the ultimate goal to promote adhesion of cells or biomolecules for tissue engineering applications.[7,8] Catechol functionalities can be introduced by immersing material substrates in an alkaline solution of 3,4-dihydroxyphenethylamine (dopamine). Thereby a thin polydopamine film is formed that exhibits reactivity towards nucleophiles, such as thiols and amines.[9–11] Polydopamine modified materials can also be used to immobilize extracellular matrix (ECM) proteins, such as collagen type I[12] or serum proteins.[11] To create polydopamine coatings on biomaterials, a large amount of dopamine is needed. To prevent the use of excessive dopamine, catechols can be directly coupled to synthetic polymers using dopamine or 3,4-dihydroxyhydrocinnamic acid, resulting in the formation of amide bonds. Brubaker et al. coupled catechols to a 4-arm poly(ethylene glycol) (PEG) and incorporated an elastase-specific peptide sequence to create an enzymatically degradable and adhesive hydrogel.[13] Subcutaneous injection of this adhesive hydrogel in mice showed slow degradation via elastase secreted by neutrophils, which minimized an inflammatory response.[13] Furthermore, Lee et al. conjugated catechol residues to the backbone of alginate, to develop biocompatible 3D hydrogel for cell transplantation.[14] By exposing the catechol modified alginate to a mixture of sodium hydroxide and sodium periodate, a divalent cation-free alginate hydrogel was created that showed a high degree of viability and low immunogenicity. Kim et al. simultaneously electrospun catechol-modified 8-arm PEG with thiolated

[a] *Institute for Complex Molecular Systems, Eindhoven University of Technology, De Zaale, 5612 AJ Eindhoven, The Netherlands*
[b] *Department of Biomedical Engineering, Laboratory for Cell & Tissue Engineering, Eindhoven University of Technology, P.O box 513, 5600 MB Eindhoven, The Netherlands*
[c] *Department of Biomedical Engineering, Laboratory of Chemical Biology, Eindhoven University of Technology, P.O. box 513, 5600 MB Eindhoven, The Netherlands*
[d] *SyMO-Chem BV, Eindhoven University of Technology, De Zaale, 5612 AZ Eindhoven, The Netherlands*

Electronic Supplementary Information (ESI) available: [details of any supplementary information available should be included here]. See DOI: 10.1039/x0xx00000x

poly(lactic-*co*-glycolic acid) and either formed a cross-linked nanofibrous network after exposure to sodium periodate solution, or formed non cross-linked meshes without exposure to sodium periodate.[15] Electrospun catechol cross-linked meshes showed improved anti-fouling properties compared to non-cross-linked meshes, due to the slower degradation rate of tethered PEG chains. Finally, Choi et al. covalently immobilized 3,4-dihydroxyhydrocinnamic acid to amines on the surface of poly(ε-caprolactone)-PEG electrospun nanofibers.[16] After exposure to basic pH, a low concentration of catechols was able to induce increased fibroblast adhesion at the surface of nanofibers (catechol concentration = 106 pmol/mm^2). In general, these findings show an enhanced cellular adhesion attributed to the conjugation of catechol-molecules to polymers. Yet, since these methods require multiple reaction steps for functionalization of material surfaces, new approaches that limit the use of excessive conjugation reactions are highly desirable.

In this study, the feasibility of supramolecular biomaterials to support cardiac tissue engineering by cardiomyocyte progenitor cells (CMPC) is studied. Cardiac tissue engineering implies the *in vitro* production of cardiac specific tissue, e.g. for cardiac repair following a myocardial infarction.[17,18] Cardiac stem/progenitor cells have the potential to regenerate cardiac tissue and provide a long term solution for cardiac tissue damage when used as a cell-therapy.[19,20] However, it remains a challenge to improve the engraftment and survival of these progenitor cells following implantation. For this reason, new synthetic biomaterials are designed such that they recapitulate the native cardiac microenvironment which improve the outcome of *in vitro* cardiac tissue engineering and *in vivo* engraftment and survival.

Here, a supramolecular approach is employed based on a combination of UPy-functionalities and mussel-inspired catechol chemistry to develop improved cell-adhesive biomaterials. For this purpose, a new UPy-based hydrophobic polymer is developed, based on priplast, that has non-cell adhesive properties. Next to this, improved cellular adhesion by catechols is studied on UPy-modified polycaprolactone polymers. Next, the goal is to modularly bioactivate both cell- and non-cell adhesive UPy-based surfaces without the use of large amounts of catechol molecules. UPy-based approaches to selectively functionalize biomaterials have previously shown to improve cellular adhesion with UPy-peptides or prevent cellular adhesion with UPy-modified poly(ethylene glycol).[21–24] In this study, adhesive mussel-inspired supramolecular biomaterials are developed, to improve CMPC-material interactions in terms of adhesion, viability and preservation of endogenous ECM formation.

Materials & methods

Materials and synthetic procedure

Bifunctional UPy-modified polycaprolactone (UPy-PCL, M_n = 2.7 kg/mol) was synthesized similar to previous methods.[21] Bifunctional UPy-modified priplast3196 (UPy-PP, MW = 3.29 kg/mol) was synthesized by reacting dihydroxyl-terminated priplast3196 with hexamethylene diisocyanate (HDI)-activated UPy using dibutyltin dilaurate (DBTDL) as a catalyst in $CHCl_3$ (Scheme S1). Monofunctionalized UPy-catechol (UPy-DOPA) was synthesized by coupling 3,4-dihydroxyphenethylamine to carboxylic acid terminated UPy-building blocks (Scheme S2).[25] General materials and instrumentations used in this study are described in the supporting information.

Preparation and analysis of dropcast films

Polymer solutions were prepared by mixing UPy-PCL (31.8 mg/ml in HFIP) or UPy-PP (38.8 mg/ml in $CHCl_3$) with UPy-DOPA (1.67 mg/ml in $CHCl_3$:MeOH (95:5)), resulting in mixtures with 10 mol% UPy-DOPA. UPy-PCL and UPy-PP based films were prepared by dropcasting 40 µL and 80 µL polymer solutions on untreated glass coverslips and silanized glass coverslips (Supporting information 1.3), respectively. Dropcast films were dried in vacuum at room temperature overnight. Fibronectin-coated coverglasses were prepared by incubating them in 30 µg/mL fibronectin in PBS for 1-2 hours. Atomic force microscopy (AFM) phase and height images of dropcast films were recorded at room temperature using a Digital Instruments Multimode Nanoscope IV operating in the tapping regime mode using silicon cantilever tips (PPP-NCHR, 204-497 kHz, 10-130 N/m). Images were processed using Gwyddion software (version 2.43). Water contact angles were measured on an OCA30 (DataPhysics) at room temperature. Water droplets (4 µL) were applied on the dropcast films and the angle of the water-air-polymer interface was measured after 30 seconds. Arnow's test was performed to detect catechol residues within the dropcast films.[26] In this assay, the following components are sequentially added to produce a red/brown color in the presence of phenolic hydroxyl groups: 0.5 mL HCl (0.5 M), 0.5 mL nitrite-molybdate (0.02 v/v%), 0.5 mL NaOH (1 M), and 0.5 mL distilled water. Images were taken with a digital camera (…) and contrast was manually adapted to highlight the differences between UPy-PP films without and with UPy-DOPA or UPy-PCL films without and with UPy-DOPA.

Cell culture

L9TB cardiomyocyte progenitor cells (CMPC) were immortalized by lentiviral transduction of hTert and BMI-1 (L9TB).[27] CMPCs were cultured in SP++ growth medium containing M199 (Gibco) and EGM-2 (Lonza) in a 3:1 ratio, supplemented with 10% fetal bovine serum, 1% penicillin/streptomycin (Lonza) and 1% non-essential amino acids (Gibco). CMPCs were cultured on 0.1% gelatin coated PS, passaged at 80-90% confluency and seeded at a concentration of 2.6x10^4 cells/cm^2.

Immunofluorescent staining

CMPCs cultured on dropcast films were fixated in 3.7% formaldehyde (Merck) for 10 minutes, washed with PBS and permeabilized with 0.5% Triton X-100 (Merck) for 10 minutes.

Non-specific binding of antibodies was minimized by incubating twice in 1% horse serum for 10 minutes. Cells were then incubated with the primary antibody in 10% horse serum and Net-gel (50 mM Tris pH7.4, 150 mM NaCl, 5 mM EDTA, 0.25% gelatin in milliQ) overnight at 4 °C. Subsequently, cells were first washed with Net-gel and incubated with the secondary antibody for 1 hour in Net-gel followed by incubation with DAPI (0,1 µg/mL) in PBS for 5 minutes. Finally, samples were washed and mounted on cover glasses with mowiol (Sigma). Information regarding, primary and secondary antibodies are listed in the supporting information. Samples were imaged with a confocal laser scanning microscope (Zeiss LSM510 META NLO).

Viability assay and collagen staining

Viability assay was performed using Calcein-AM (Fluka) and propidium iodide (PI, Invitrogen). CMPCs cultured on dropcast films were incubated with serum-free medium with 10 µM Calcein-AM and PI for 30 minutes and imaged using a fluorescent microscope (Zeiss Axiovert 200M). Cells were quantified using Mathematica software (Wolfram). Collagen was stained using a CNA35 probe linked to an mCherry dye (CNA35-mCherry).[28] Cells were incubated with 1 µM CNA35-mCherry in standard culture medium for 30 minutes and imaged using a confocal laser scanning microscope (Leica TCS SP5X).

Gene expression analysis

CMPCs were cultured for 7 days on UPy-PCL, UPy-PCL + 10 mol% UPy-DOPA and UPy-PP + 10 mol% UPy-DOPA and compared to CMPCs cultured on fibronectin-coated cover glass. Total RNA was isolated using the Qiagen RNAeasy isolation kit (Qiagen). cDNA was synthesized for 250 ng RNA per sample using the MMLV (Bio-Rad). Primers for quantitative PCR (qPCR) were designed using qPrimerDepot[29] and BLAST. cDNA samples were subjected to qPCR using iQTM SYBR@ Green Supermix (Bio-Rad) and the Bio-Rad IQ^{TM}5 detection system (Version 1.6). Primer sequences and annealing temperatures can be found in the supporting information.

Statistical analysis

Data are presented as mean ± standard deviation (SD). These data consisted of water contact angles, cellular adhesion, viability and relative gene expression. All statistical differences were determined using a non-parametric Kruskal-Wallis test with Dunn's post-hoc test. Probabilities of $p<0.05$ were considered as significantly different. All statistical analyses were performed using GraphPad Prism 5 Software (GraphPad Software, Inc.)

Results & discussion

Successful synthesis of UPy modules

Hydrophobic priplast polymers were end-functionalized with UPy groups to yield an elastic material (glass transition temperature T_g = -51.9 °C, T_c = 37.1 °C (ΔH = 4 J/g), T_m = 77.3 °C (ΔH = 5.6 J/g)) (Scheme 1). Synthesis of UPy-modified catechol functionalities (UPy-DOPA) was successfully achieved by employing a peptide coupling strategy (Scheme S2).[25]

Bioactive supramolecular elastomers are successfully formulated

Supramolecular assembly of the mixtures was investigated with AFM on dropcast films (Figure 1A). Short and regular fibers can be observed on UPy-PP films at the nanometer scale (Figure 1A), which originates from the hydrogen bonding of the UPy groups and lateral stacking of UPy-dimers.[30] However, UPy-PP fibers are shorter compared to UPy-PCL dropcast films, which is due to the lower hydrogen bonding potential of the urethane spacer in the backbone of UPy-PP in contrast to the urea spacer in the backbone of UPy-PCL (Scheme 1).[31] Upon mixing 10 mol% UPy-DOPA with UPy-PP, a similar fibrous morphology can be observed (Figure 1A). This indicates successful incorporation of UPy-DOPA within the UPy-stacks of UPy-PP. Additionally, similar height distribution can be observed for UPy-PP and UPy-PP with UPy-DOPA, which also indicates successful incorporation of UPy-DOPA within UPy-PP fibers (Figure S1A and B). Furthermore, long and regular fibers can be observed on UPy-PCL at the nanometer scale (Figure 1A), which is similar with previous dropcast films of UPy-PCL.[32] Upon mixing 10 mol% UPy-DOPA with UPy-PCL, a similar fiber morphology can be observed, which indicates successful incorporation of UPy-DOPA within the base material (Figure 1A). Similar height distribution can be observed for both UPy-PCL based dropcast films (Figure S1C and D). No difference in hydrophilicity was observed when 10 mol% UPy-DOPA was mixed with either pristine polymers UPy-PP (89.6±0.8 vs 90.0±0.6, with and without UPy-DOPA, respectively) or UPy-PCL (69.9±1.0 vs 68.5±0.8, with and without UPy-DOPA, respectively), based on WCA measurements (Figure 1B). This is in contrast with previous reports, where a significant decrease in WCA was observed after modification of hydrophobic surfaces with catechol molecules via polydopamine.[11] This could be due to higher amount of catechols used to modify material surfaces. To determine the presence of catechol functionalities in the dropcast films, an arnow's test was performed (Figure 1C). A clear red/brown color change was observed for dropcast films containing UPy-DOPA, which indicates the presence of oxidated catechol moieties. These results show the successful bioactivation of UPy-based materials using UPy-DOPA.

Adhesion and viability is improved following bioactivation

Incorporation and bioactivity of UPy-DOPA within pristine UPy-based polymers was tested at a cellular level by investigating CMPC adhesion after 24 hours of culturing (Figure 2A). On UPy-PP CMPCs did not adhere after 24 hours (Figure 2A). Upon increase in concentration of UPy-DOPA, an increase in CMPC adhesion is observed for 5 mol% and 10 mol%. This matches with the total amount of cells per mm^2, which significantly increases to 170.9±13.4 for 5 mol% and 147.9±29.9 for 10 mol% UPy-DOPA (Figure 2B). The increase in adhesion and cell

number is either due to, i) an increase in the number of bound serum proteins or ii) an increase in the adsorption strength of serum proteins on UPy-PP. In literature, improved adhesion on catechol-functionalized surfaces is interpreted by the ability to immobilize thiol/amine containing biomolecules via Michael-Type addition or Schiff-base reactions to *o*-quinones.[16] In this study, no sodium periodate or basic solutions were used, which are required to oxidize catechols to reactive *o*-quinones.[33] Furthermore, on hydrophobic surfaces, proteins tend to denature and therefore they might lose some of their adhesive properties.[34] Further analysis is needed to test whether surface bound serum proteins denature or if the surface of UPy-PP films prevents the adsorption of serum proteins. As a control group, both UPy-PP and UPy-PCL were functionalized with UPy-MeO, an analogue guest molecule lacking catechol functionality, to confirm the effect of catechols at the surface (Figure S3). On UPy-PP functionalized with UPy-MeO, no improvement in the adhesion of CMPCs was observed, proving the effect of catechol functionalities that improve cellular adhesion on UPy-PP films (Figure S4). On pristine UPy-PCL CMPCs show adhesion and spreading (Figure 2A). This is in agreement with previous studies where 3T3 fibroblasts showed adhesion and spreading when cultured on pristine UPy-PCL.[21] CMPCs show a slight increase in spreading upon increase in molar concentration of UPy-DOPA to 10 mol%. Additionally, the amount of cells per mm^2 slightly increased upon increase of UPy-DOPA concentration, however not significantly (Figure 2C). Similarly, UPy-PCL functionalized with UPy-MeO showed no improvement of cell adhesion (Figure S5). Next, viability of CMPC was assessed on UPy-based films after 24 hours of culturing (Figure 2D and S6). On UPy-PP CMPCs showed low viability (16.5±3.1%), which is primarily due to the loss of cellular adhesion after 24 hours of culturing. Upon incorporation of UPy-DOPA CMPC adhesion significantly increased (90.4±4.1%). On UPy-PCL CMPCs showed high viability and upon incorporation of UPyDOPA, viability remained unchanged (97.7±1.7% and 98.6±0.6%, respectively) (Figure 2D). However, the absolute number of adhered cells did increase upon incorporation of 10 mol% UPy-DOPA (data not shown). Successful improvement of CMPC adhesion was achieved by modularly incorporating low amounts of UPy-DOPA (1.67 mg/ml) in UPy-based polymers, excluding the use of oxidating agents or basic pH.

Cardiac ECM gene expression is preserved

Recently, CMPCs have proven to be a potential cell source for cardiac tissue engineering approaches due to their ability to proliferate, differentiate into cardiomyocytes and their capacity to produce cardiac ECM components.[27,35,36] To test the ECM formation capabilities of CMPCs on different supramolecular surfaces, cardiac specific ECM gene expression is studied. For simplification, the cardiac ECM was divided into three categories, 1) the pericellular matrix, 2) basement membrane and 3) connective tissue layer (Figure 3A). The pericellular matrix consists of hyaluronan and proteoglycan link protein 3 (HAPLN3) and versican (VCAN). The basement membrane consists of collagen type IV (COL4A1), proteoglycan α-1 (HSPG2), laminin γ-1 (LAMC1) and nidogen (NID1). Finally, the connective tissue layer consists of fibrillin-1 (FBN1), collagen type III (COL3A1), decorin (DCN), collagen type I (COL1A1) and fibronectin (FN1). Gene expression of CMPCs cultured for 7 days on the different supramolecular surfaces were compared to CMPCs cultured on fibronectin-coated glass to check the effect of the supramolecular surface on gene expression levels (Figure 3B-D). Due to high cell death on pristine UPy-PP surfaces, gene expression was impossible to be measured for this condition (Figure 2D). On UPy-PP functionalized with UPy-DOPA low gene expression for the ECM components HAPLN3, COL4A1, DCN and COL1A1 can be seen compared to CMPCs cultured on fibronectin-coated cover glass (Figure 3D). This might be due to the lower amount of CMPCs on UPy-PP based films compared to UPy-PCL based films after 7 days of culture (data not shown). Nevertheless, cardiac markers which are identical for CMPC are expressed and maintained on all surfaces (Figure S7). On pristine UPy-PCL, genes expressed for ECM components found in the pericellular matrix, basement membrane and connective tissue layer, showed similar levels of expression compared to CMPCs cultured on fibronectin-coated glass (Figure 3B). Similarly, on UPy-DOPA functionalized UPy-PCL films, gene expression of all cardiac categories remained similar compared to CMPCs cultured on fibronectin-coated glass (Figure 3C). These results show the feasibility to maintain CMPC-based cardiac ECM formation through the preservation of ECM gene expression and CMPC phenotype on catechol-functionalized supramolecular surfaces.

Cardiac ECM production is preserved

Cardiac specific protein production and localization on supramolecular surfaces and the effect of catechol incorporation is studied (Figure 4). Similarly, due to high cell death on pristine UPy-PP surfaces, ECM production was impossible to be measured (Figure 2D). The basement membrane component laminin γ1 was located in small quantities in the cytosol (Figure 4A, 4F and 4K). Similarly, collagen IV was observed in low amounts on all surfaces (Figure 4B, 4G and 4L). High amounts of extracellular fibronectin was seen on all surfaces, however no difference was observed when catechol functionalities were incorporated (Figure 4C, 4H and 4M). Further analysis should be performed to assess fibronectin immobilization on catechol-functionalized supramolecular surfaces. Since fibronectin production is a crucial ECM component which has been shown to improve matrix assembly and cardiac progenitor cell proliferation and alignment.[37,38] Furthermore, high amounts of extracellular collagen type I was observed on all surfaces (Figure 4D, 4I and 4N). Additionally, collagen production was visualized with CNA35-mCherry, where high amounts of extracellular collagen can be observed on all surfaces (Figure S8).[39] Lastly, collagen type III was mostly observed within the cytosol of CMPCs (Figure 4E, 4J and 4O). With these results, it can be concluded

that ECM production by CMPCs is preserved on catechol-functionalized supramolecular surfaces.

Conclusions

Successful formulation and development of adhesive supramolecular surfaces using UPy-DOPA was achieved. This was realized by modularly incorporating UPy-DOPA with non-cell adhesive UPy-PP and cell-adhesive UPy-PCL, thereby, creating improved cellular adhesive supramolecular biomaterials. Additionally, these supramolecular biomaterials showed the capability to support the preservation of endogenous ECM gene and protein expression by CMPCs, which is of high relevance for cardiac tissue engineering approaches.

Acknowledgements

Marie-José Goumans is gratefully acknowledged for the L9TB CMPC. We acknowledge the support from the Netherlands Cardiovascular Research Initiative (CVON 2012-01): The Dutch Heart Foundation, Dutch Federation of University Medical Centers, the Netherlands Organization for Health Research and Development and the Royal Netherlands Academy of Sciences. Additionally, this work was financially supported by the European Research Council (FP7/2007-2013) ERC Grant Agreement 308045, the Ministry of Education, Culture and Science (Gravity program 024.001.03), and ZonMW as part of the LSH 2Treat program (project number 436001003).

Notes and references

1 K. Autumn, Y. A. Liang, S. T. Hsieh, W. Zesch, W. P. Chan, T. W. Kenny, R. Fearing and R. J. Full, *Nature*, 2000, **405**, 681–685.

2 H. Lee, B. P. Lee and P. B. Messersmith, *Nature*, 2007, **448**, 338–341.

3 M. D. Bartlett, A. B. Croll and A. J. Crosby, *Adv. Funct. Mater.*, 2012, **22**, 4985–4992.

4 R. J. Stewart, T. C. Ransom and V. Hlady, *J. Polym. Sci. Part B Polym. Phys.*, 2011, **49**, 757–771.

5 N. K. Kaushik, N. Kaushik, S. Pardeshi, J. G. Sharma, S. H. Lee and E. H. Choi, *Mar. Drugs*, 2015, **13**, 6792–6817.

6 L. Li, W. Smitthipong and H. Zeng, *Polym. Chem.*, 2015, **6**, 353–358.

7 C. E. Brubaker and P. B. Messersmith, *Langmuir*, 2012, **28**, 2200–2205.

8 S. K. Madhurakkat Perikamana, J. Lee, Y. Bin Lee, Y. M. Shin, E. J. Lee, A. G. Mikos and H. Shin, *Biomacromolecules*, 2015, **16**, 2541–2555.

9 H. Lee, S. M. Dellatore, W. M. Miller and P. B. Messersmith, *Science*, 2007, **318**, 426–430.

10 Y. M. Shin, I. Jun, Y. M. Lim, T. Rhim and H. Shin, *Macromol. Mater. Eng.*, 2013, **298**, 555–564.

11 S. H. Ku, J. Ryu, S. K. Hong, H. Lee and C. B. Park, *Biomaterials*, 2010, **31**, 2535–2541.

12 N. Li, G. Chen, J. Liu, Y. Xia, H. Chen, H. Tang, F. Zhang and N. Gu, *ACS Appl. Mater. Interfaces*, 2014, **6**, 17134–43.

13 C. E. Brubaker and P. B. Messersmith, *Biomacromolecules*, 2011, **12**, 4326–4334.

14 C. Lee, J. Shin, J. S. Lee, E. Byun, J. H. Ryu, S. H. Um, D. I. Kim, H. Lee and S. W. Cho, *Biomacromolecules*, 2013, **14**, 2004–2013.

15 H. S. Kim, H. O. Ham, Y. J. Son, P. B. Messersmith and H. S. Yoo, *J. Mater. Chem. B*, 2013, **1**, 3940–3949.

16 J. S. Choi, P. B. Messersmith and H. S. Yoo, *Macromol. Biosci.*, 2014, **14**, 270–279.

17 Y. S. Zhang, J. Aleman, A. Arneri, S. Bersini, F. Piraino, S. R. Shin, M. R. Dokmeci and A. Khademhosseini, *Biomed. Mater.*, 2015, **10**, 34006.

18 L. A. Reis, L. L. Y. Chiu, N. Feric, L. Fu and M. Radisic, *J. Tissue Eng. Regen. Med.*, 2016, **10**, 11–28.

19 P. Goichberg, J. Chang, R. Liao and A. Leri, *Antioxid Redox Signal*, 2014, **21**, 2002–2017.

20 S. Koudstaal, S. J. Jansen of Lorkeers, R. Gaetani, J. M. I. H. Gho, F. J. van Slochteren, J. P. G. Sluijter, P. A. Doevendans, G. M. Ellison and S. A. J. Chamuleau, *Stem Cells Transl. Med.*, 2013, **2**, 434–443.

21 P. Y. W. Dankers, M. C. Harmsen, L. a Brouwer, M. J. A. Van Luyn and E. W. Meijer, *Nat. Mater.*, 2005, **4**, 568–574.

22 B. B. Mollet, M. Comellas-Aragonès, a. J. H. Spiering, S. H. M. Söntjens, E. W. Meijer and P. Y. W. Dankers, *J. Mater. Chem. B*, 2014, **2**, 2483.

23 G. C. Van Almen, H. Talacua, B. D. Ippel, B. B. Mollet, M. Ramaekers, M. Simonet, A. I. P. M. Smits, C. V. C. Bouten, J. Kluin and P. Y. W. Dankers, *Macromol. Biosci.*, 2016, **16**, 350–362.

24 A. C. H. Pape, B. D. Ippel and P. Y. W. Dankers, *Langmuir*, 2017, **0**, acs.langmuir.7b00467.

25 I. De Feijter, O. J. G. M. Goor, S. I. S. Hendrikse, M. Comellas-Aragonès, S. H. M. Söntjens, S. Zaccaria, P. P. K. H. Fransen, J. W. Peeters, L. G. Milroy and P. Y. W. Dankers, *Synlett*, 2015, **26**, 2707–2713.

26 L. E. Arnow, *Comp. A J. Comp. Educ.*, 1937, 531–537.

27 A. M. Smits, P. van Vliet, C. H. Metz, T. Korfage, J. P. G. Sluijter, P. A. Doevendans and M.-J. Goumans, *Nat. Protoc.*, 2009, **4**, 232–243.

28 S. J. A. Aper, A. C. C. Van Spreeuwel, M. C. Van Turnhout, A. J. Van Der Linden, P. A. Pieters, N. L. L. Van Der Zon, S. L. De La Rambelje, C. V. C. Bouten and M. Merkx, *PLoS One*, 2014, **9**, 1–21.

29 W. Cui, D. D. Taub and K. Gardner, *Nucleic Acids Res.*, 2007, **35**, D805–D809.

30 W. P. J. Appel, G. Portale, E. Wisse, P. Y. W. Dankers and E. W. Meijer, *Macromolecules*, 2011, **44**, 6776–6784.

31 H. Kautz, D. J. M. Van Beek, R. P. Sijbesma and E. W. Meijer, *Macromolecules*, 2006, **39**, 4265–4267.

32 E. Wisse, A. J. H. Spiering, P. Y. W. Dankers, B. Mezari, P. C. M. M. Magusin and E. W. Meijer, *J. Polym. Sci. Part A Polym. Chem.*, 2011, **49**, 1764–1771.

33 J. Yang, M. A. Cohen Stuart and M. Kamperman, *Chem. Soc. Rev.*, 2014, **43**, 8271–8298.

34 J. li Zhai, L. Day, M. I. Aguilar and T. J. Wooster, *Curr. Opin.*

Colloid Interface Sci., 2013, **18**, 257–271.
35 N. A. M. Bax, M. H. van Marion, B. Shah, M.-J. Goumans, C. V. C. Bouten and D. W. J. van der Schaft, *J. Mol. Cell. Cardiol.*, 2012, **53**, 497–508.
36 M. H. van Marion, N. A. M. Bax, M. C. van Turnhout, A. Mauretti, D. W. J. van der Schaft, M. J. T. H. Goumans and C. V. C. Bouten, *J. Mol. Cell. Cardiol.*, 2015, **87**, 79–91.
37 A. Hielscher, K. Ellis, C. Qiu, J. Porterfield and S. Gerecht, *PLoS One*, 2016, **11**, e0147600.
38 K. M. French, J. T. Maxwell, S. Bhutani, S. Ghosh-Choudhary, M. J. Fierro, T. D. Johnson, K. L. Christman, W. R. Taylor and M. E. Davis, *Stem Cells Int.*, 2016, **2016**, 1–11.
39 J. Glowacki and S. Mizuno, *Biopolymers*, 2008, **89**, 338–344.

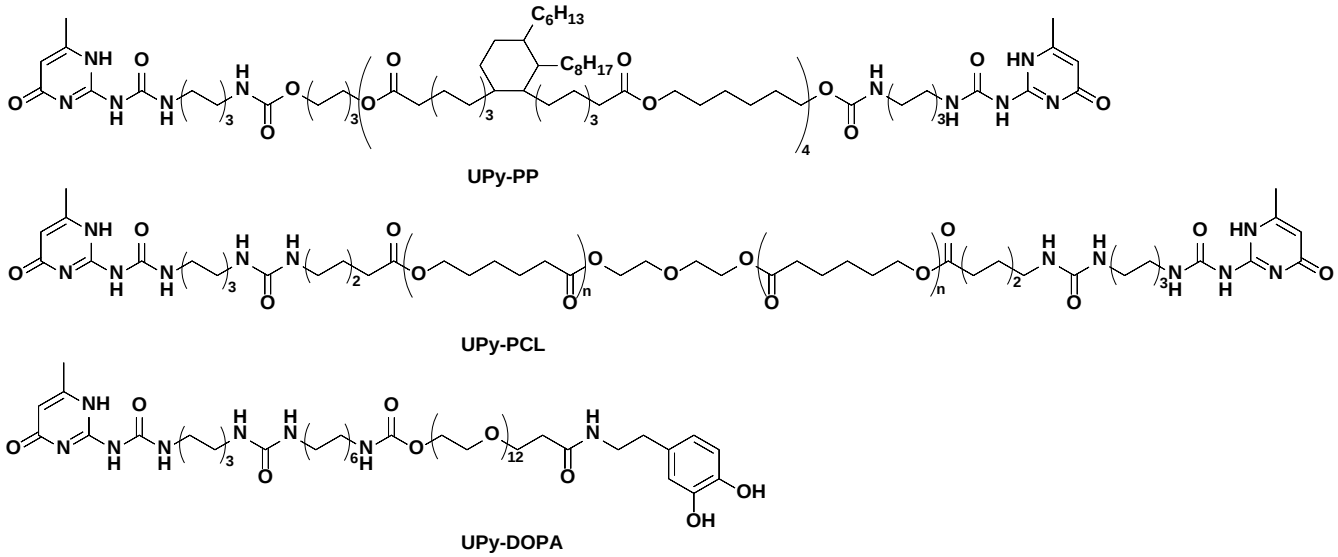

Scheme 1: Chemical structures of UPy compounds. Priplast end-functionalized with UPy-unit (**UPy-PP**), polycaprolactone end-functionalized with UPy-unit (**UPy-PCL**) and UPy-modified catechol functionalities (**UPy-DOPA**).

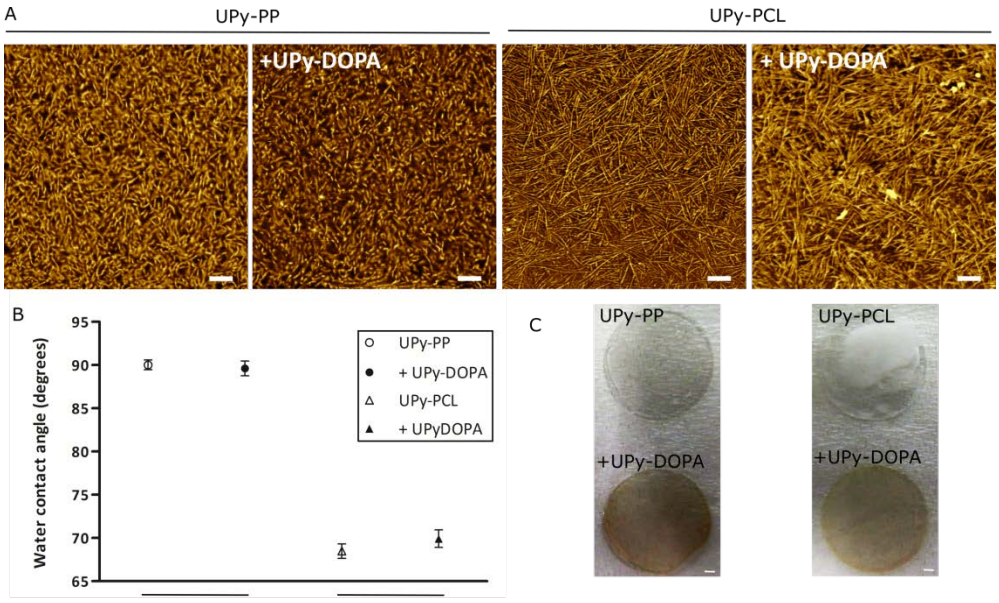

Figure 1: Material characterization of dropcast films. (A) Atomic force microscopy phase images of dropcast films consisting of UPy-PP without (left) and with 10 mol% UPy-DOPA (right), UPy-PCL without (left) and with 10 mol% UPy-DOPA (right). Scale bar is equal to 100 nm. (B) Water contact angles in degrees after 30s on dropcast films (n=6). (C) Arnow's test to check for the presence of catechol functionalities in dropcast films. Scale bar is equal to 1 mm.

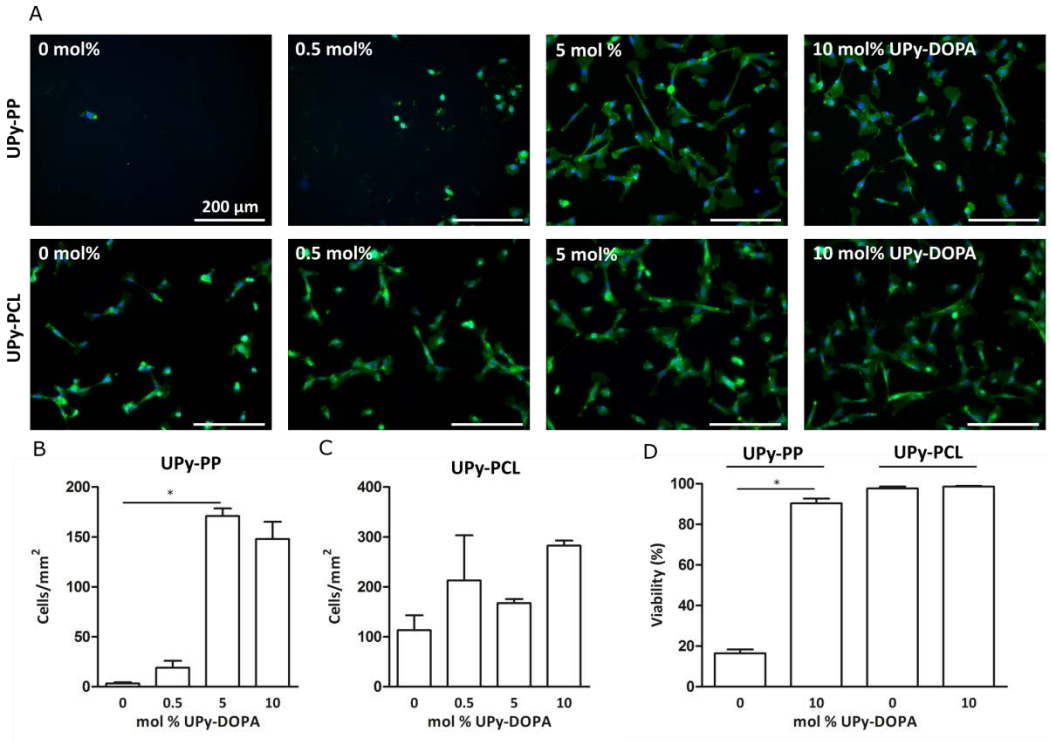

Figure 2: CMPC adhesion after culturing for 1 day on dropcast films. (A) Immunofluorescence micrographs showing adhesion of CMPC with increasing mol% UPy-DOPA in base polymer UPy-PP and UPy-PCL in the top and bottom row, respectively. Integrin-β1 (green) and nucleus (blue). Scale bar is equal to 200 µm. (B, C) Quantification of the amount of cells/mm^2 with increasing mol% UPy-DOPA in base polymer UPy-PP and UPy-PCL in the left and right graph, respectively. (D) Graph showing the viability of CMPC after 1 day on UPy-PP and UPy-PCL and after the addition of UPy-DOPA. (n=3)

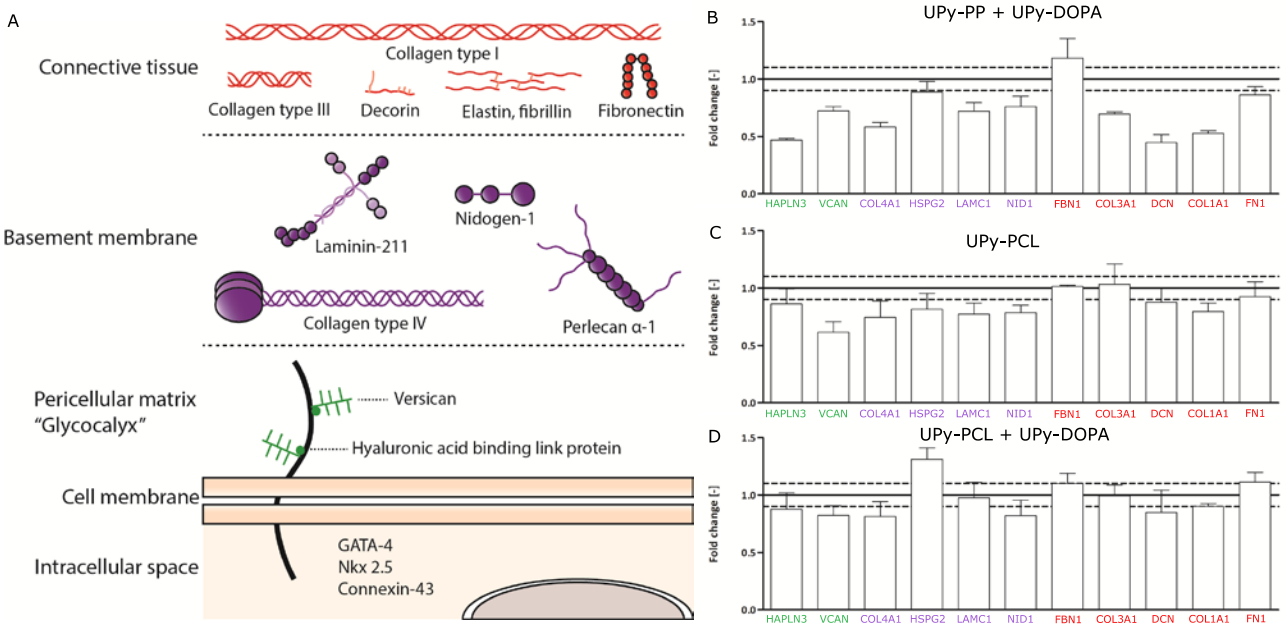

Figure 3: Expression of ECM genes by CMPC. (A) Overview of cardiac-specific ECM components and are arranged in pericellular matrix in red (Versican and HAPLN3), Basement membrane in purple (Nidogen-1, Laminin γ1, perlecan α1 and Collagen IV) and Connective tissue in red (Fibronectin, Collagen I, Decorin and Collagen III). (B-D) Gene expression by CMPC after culturing for 7 days on UPy-PCL, UPy-PCL with 10 mol% UPy-DOPA and UPy-PP with 10 mol% UPy-DOPA compared to CMPC cultured on fibronectin-coated glass. Relative gene expression of corresponding ECM component on (B) UPy-PP + UPy-DOPA, (C) UPy-PCL and (D) UPy-PCL + UPy-DOPA compared to expression of CMPC cultured on fibronectin-coated glass which is normalized to 1, represented by straight (mean) and dotted (SD) line. Bars represent means+SD. (n=3)

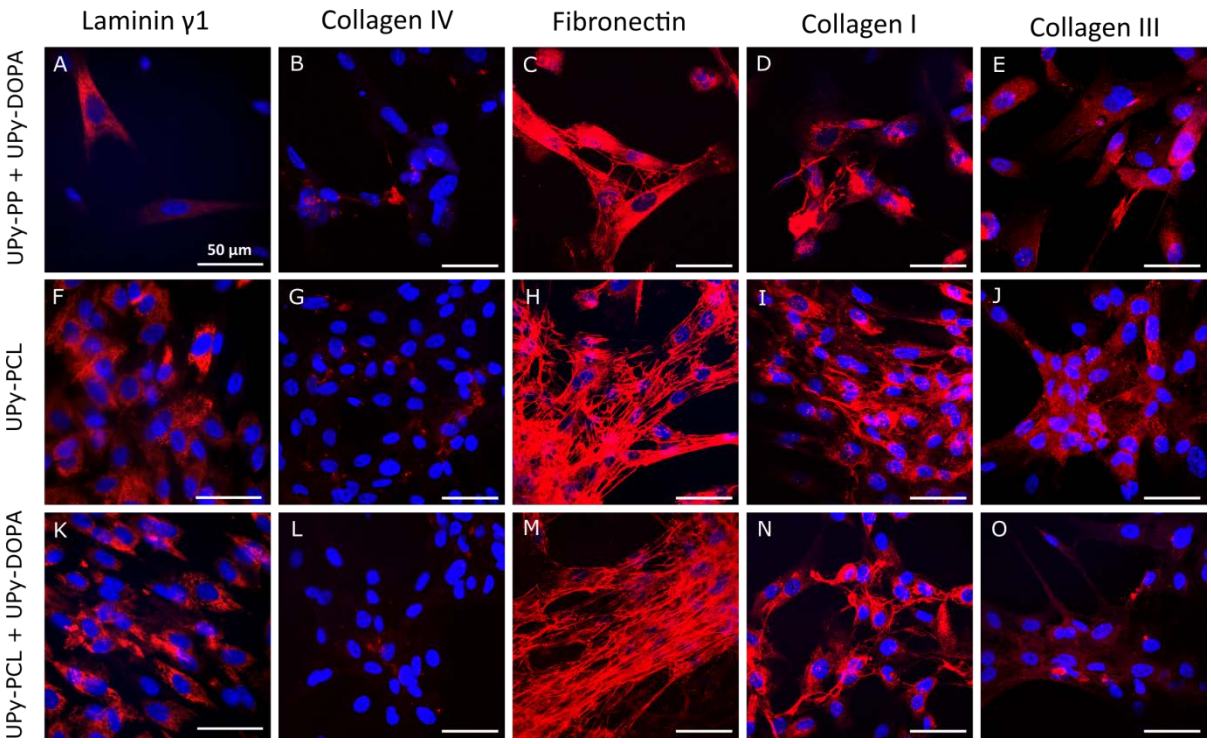

Figure 4: Immunofluorescence micrographs showing ECM production by CMPC after culturing for 7 days on dropcast films. ECM production is visualized on (A-E) UPy-PP + 10 mol% UPy-DOPA, (F-G) UPy-PCL and (K-O) UPy-PCL + 10 mol% UPy-DOPA. ECM component are (A,F,K) laminin γ1, (B,G,L) collagen IV, (C,H,M) fibronectin, (D,I,N) collagen I and (E,J,O) collagen III. ECM components are presented in red and nucleus in blue. Scale bar = 50 µm.